FIELD AND LABORATORY ASSESSMENT OF CRACKING DAMAGE FROM ALKALI-AGGREGATE REACTIONS IN CONCRETE SLABS ON GROUND, COLUMN FOOTINGS AND PERIMETER FOUNDATIONS, MIDWEST USA

David Rothstein[1*], Ramon L. Carrasquillo[2], Carlos Garza[2]

[1] DRP Consulting, Inc., Boulder, Colorado

[2] Carrasquillo Associates, Ltd., Austin, Texas

Abstract

Condition surveys and petrographic examinations indicate that cracking damage in cast in place concrete construction elements from a correctional facility in the midwestern US is from alkali-carbonate reaction (ACR) in the coarse aggregate. Traces of alkali-silica reaction (ASR) were observed involving the fine aggregate, but no damage was linked to ASR. Accelerated exposure tests using variably concentrated NaOH solutions at 80ºC assessed the potential for additional cracking. Significant ASR was observed for solutions with 0.50 N NaOH and above with no increase in cracking from ACR. A second phase of work showed that cracking increased over the eighteen months following the initial surveys. Petrographic damage rating indices (DRI) showed that the increase in cracking damage was from ACR and that ASR damage mechanisms observed in the accelerated tests were insignificant in the field. These results were used to formulate recommendations to rehabilitate the structure.

Keywords: petrography, accelerated testing, damage rating index

1 INTRODUCTION

Although the recognition of alkali-aggregate reaction (AAR) is relatively straightforward, owners of facilities affected by AAR face a multitude of questions once it is detected. The most basic is whether the concrete requires repair or not. In many cases, alkali-silica reaction (ASR) may be present but it does not impact the performance of the concrete [1]. When damage from AAR does impact performance, understanding the remaining service life becomes central to developing technically sound and economically viable strategies to deal with the rehabilitation of the structure. Some structures may require immediate and major repairs, while vigilant moisture management may prolong serviceability for years before major repairs are needed in other structures. However, predicting the rate at which damage will progress in real structures affected by AAR remains a difficult problem, even with significant advances in our understanding of AAR mechanisms [1] and the development of predictive models from numerical and experimental methods [2]. This presents a significant challenge to owners to provide sound bases for managing the fiscal burdens of repairs.

This paper describes a study that evaluated the severity of damage in a concrete structure affected by both alkali-carbonate reaction (ACR) and ASR. The study shows how combining field work, petrography, and accelerated laboratory test methods provided the information needed to make sound engineering judgements regarding the serviceability of structures affected by AAR and to formulate methods to rehabilitate such structures.

* Correspondence to: petro@drpcinc.com

2 BACKGROUND AND METHODS

2.1 Background

The study involves a forensic investigation of a correctional facility in the midwestern United States. The construction elements include reinforced concrete slabs-on-ground with continuous cast-in-place concrete footings, reinforced concrete masonry unit (CMU) walls, steel columns supported by individual concrete footings, and continuous concrete footings along the perimeter fences. No information regarding the concrete mix designs or data from testing during construction were available for the investigation. Distress originally manifested as map cracking in exterior concrete slabs-on-ground within three years of the original construction. The distress became more severe with time and began to affect other elements at the facility, resulting in cracking of the exterior CMU walls and deflection of exterior fence posts.

2.2 Methods for assessment and analysis

General

The investigation involved detailed condition surveys of the existing as-built structure, concrete core sampling, petrographic examination, and accelerated exposure testing.

Condition surveys and sampling

The site was visited four different times over an eighteen-month period. During these visits activities included condition assessments, photographic documentation, non-destructive testing, and concrete sampling. The concrete sampling involved the extraction of more than 60 cores. The cores measured 95 mm in diameter and generally ranged from 125 mm to more than 300 mm in length. In several cases multiple cores were taken at the same locations but during different site visits. This permitted monitoring the progression of damage with time. In some cases multiple cores were taken from the same locations at the same times with companion cores set aside for the accelerated exposure testing described below.

Petrographic examination

Petrographic examinations were done on 38 cores following the procedures outlined in ASTM C856-10 [3]. Polished slabs and petrographic thin sections were prepared for reflected and transmitted light microscopy, respectively, following standard procedures [4, 5]. The polished slabs were examined with a Nikon SMZ-1500 stereomicroscope equipped to provide a magnification range from 3-180x. The thin sections were examined with a Nikon E-600 Pol polarizing microscope equipped to provide a magnification range from 50-1000x.

Measurements of damage linked to AAR were obtained using the Damage Rating Index (DRI) method [6] with weighting factors somewhat modified [e.g., 7] for the present investigation. The DRI methodology employed in this study addressed damage related to ACR in the coarse aggregate and ASR in the fine aggregate. Orthogonal microcracks in reaction rims of coarse aggregate particles were introduced as a measured feature and given a weighting factor equal to cracks in the paste. Although this feature increases the contribution of ACR to the DRI score, this is not significant because the same factors were used for all the cores and the intent was to assess changes in the DRI scores over time with an internally consistent set of analyses. Therefore, the DRI numbers obtained from this study should not be compared to other investigations to attain a sense of the degree of damage. The microscopy for the DRI was done at 20x magnification and all the DRI scores were normalized to a survey area of 120 cm^2 for each core. Table 1 summarizes the features and weighting factors used for the DRI method.

Accelerated exposure testing

The accelerated test methods were done modifying procedures outlined in ASTM C1260 [8] as follows. Six sections were cut from concrete cores selected for the exposure tests. The cores represented companions for samples that were previous subjects of petrographic examinations. The cores were cut into thirds longitudinally, providing three cross sections through each core with at least one flat surface. Each cross section was then cut in half lengthwise to provide a total of six saw-cut sections from each core. Each section was lapped and polished following identical procedures used for the petrography. The sections measured at least 75 mm in length and about 95 mm in width. One section from each core was held in reserve and the other five sections were placed in sealed reaction vessels filled with the different NaOH solutions. The strength of the solutions were 0.0, 0.25, 0.50, 0.75 and 1.0 N. The solution:sample volumes were similar to those specified in [8]. The vessels were placed in an oven maintained at 80ºC for fourteen days and then removed. No attempts were made to measure expansion with fixed pins or any other methods The sections were examined with a stereomicroscope to assess the extent of AAR.

3 RESULTS

3.1 Condition surveys

The initial condition surveys identified map cracking in exposed concrete elements such as exterior slabs on ground, exterior equipment mat concrete foundations, and on the continuous and individual fence post foundations (Figure 1). Distress in other building elements included linear, sub-vertical cracking in exterior CMU walls, the impaired operation of exterior doorways, and the deflection of perimeter fence posts. The initial surveys raised concerns regarding the integrity of the cast-in-place concrete that was not exposed, such as interior slabs on ground, which were coated, and below-grade construction elements such as the continuous footings of the structure and individual column footings. Subsequent exhumation of these below grade elements also revealed map cracking. After an 18 month hiatus, condition surveys were done on the previously surveyed areas, both above and below grade. An increase in the extent and density of map cracking was observed at virtually every location on the exterior slabs on grade. The severity of map cracking also increased along areas of the continuous exterior foundations and along individual fence post foundations. The interior slabs on ground did not show marked increases in map cracking except near exterior doorways.

3.2 Petrographic examination

General

The concrete has the following characteristics. The paste consists of hydrated portland cement and fly ash. No slag cement or other supplemental cementitious materials are present. The hydration is normal to somewhat advanced. Most of the cores are air-entrained, but a few lack entrained air. The concrete is generally well-consolidated with no significant bleed voids or consolidation voids observed. The cores show negligible carbonation (< 1 mm). Minor deposits of ettringite were commonly observed in voids.

Aggregate

The coarse aggregate is a crushed, quarried limestone with a nominal top size of 19 mm. The rocks are dense, moderately hard and evenly graded. The coarse aggregate ranged in composition from mostly dolomitic rocks to mostly calcitic rocks. This led to the designation of cores as Type A where dolomitic limestone predominated and Type B where calcitic limestone predominated. Some cores presented a mix of dolomitic and calcitic limestones (Type A/B). This suggested that the dolomitic and calcitic limestones represented different ledges within the same quarry. The dolomitic limestone has textural features typical of rocks that show susceptibility to ACR, with isolated rhombohedral crystals of dolomite set within a very fine-grained matrix consisting of carbonate and clay minerals. Evidence of de-dolomitization, where euhedral angular rhombs of dolomite grade into less well-defined crystals, was occasionally observed in reaction rims in the Type A cores.

The fine aggregate is a natural siliceous river sand that has a nominal top size of 4.75 mm. The rocks are dense and hard and evenly graded. The rocks and minerals present in the sand consist primarily of quartz, felspar and igneous rocks that range widely in composition from granitic to dioritic. Minor components include siliceous sedimentary rocks such as chalcedonic chert and quartzite, and mafic phases such as pyroxene and amphibole. Occasional particles of coal associated with surface popouts were also observed.

Alkali-Carbonate Reaction

Evidence of ACR was observed in almost all the cores. Although reaction rims were occasionally observed on coarse aggregate particles in Type B cores, no cracking, microcracking or any other distress due to ACR was observed in the Type B cores. Moderate to severe ACR with damage manifested by cracking and/or abundant microcracking was only observed in the Type A cores. Numerous features were observed on the polished surfaces from the cores that indicate ACR in the Type A cores. Macroscopic cracks ranging up to 500 μm wide and 50 mm long cut through the dolomitic limestones and the paste to significant depths in the Type A cores (Figure 2). These cracks were free of secondary deposits. Reaction rims that range up to 250 μm wide were commonly observed on the dolomitic limestone particles in all the Type A cores. Only the Type A cores showed microcracks oriented orthogonally to the paste-aggregate boundary in the coarse aggregate reaction rims (Figure 3). These microcracks were generally less than 25 μm wide and 100 μm long. Three other types of microcracks were observed in the Type A cores. These include randomly oriented microcracks that cut through the paste and reach widths of 75 μm and lengths of 6 mm, internal microcracks within coarse aggregate particles that range from 25-50 μm wide and 1-2 mm long, and microcracks ranging up to 50 μm wide and 4 mm long that cut from the interior of coarse aggregate particles into the paste. Almost all of these microcracks were free of secondary deposits.

Clear evidence of ACR was also observed in thin section (Figure 4). A few cores showed aggregate particles cut by microcracks filled with fine-grained carbonate minerals that cut from the aggregate into the paste. Deposits of brucite were observed in occasional voids near reactive aggregate particles. Some aggregate particles showed clear depletion of dolomite rhombs near the paste-aggregate boundary.

Alkali-Silica Reaction

Occasional cores of both Type A and Type B aggregate showed evidence of ASR involving chert particles in the fine aggregate (Figure 5). The evidence of ASR typically included reaction rims and internal microcracking in chert particles, with deposits of ASR gel observed in rare voids and microcracks. No evidence of cracking or significant microcracking due to ASR was observed in any core. A few chert particles showed evidence of pitting; no microcracking was observed in association with the pitting.

DRI Scores

Figure 6 shows the results of DRI evaluations from five different samples. The first two samples represent the same perimeter footing made with Type B aggregate that was sampled in early 2009 and late 2010. The third sample is from the same Type B perimeter footing and was sampled in early 2009, but was then subjected to the accelerated exposure testing using a 0.5 NaOH solution. These three cores were taken within 300 mm of each other. The fourth and fifth samples represent the same column footing made with Type A aggregate that was also sampled in early 2009 and then eighteen months later in late 2010. These cores were also taken within 300 mm of each other.

The analysis of the Type B perimeter footing cores shows that they are not affected by ACR but show evidence of negligible ASR in the fine aggregate, primarily involving reaction rims on fine aggregate particles with a few occurrences of pitting observed as well. No significant increase in the frequency of either of these features was observed in the 2010 core. Both cores presented one (1) example of an air void lined with ASR gel and neither core showed cracking or microcracking of the paste. After the accelerated exposure test, the concrete showed a marked increase in the frequency of pitting and air voids lined with gel; minor microcracking of the paste was also observed.

The analysis of the Type A column footing cores clearly demonstrated damage from ACR in the coarse aggregate. The most significant damage features include microcracks in reaction rims and cracks in the paste, but debonding and internal microcracking of the coarse aggregate was also observed. Reaction rims were observed on chert particles in the sand, albeit less frequently than in the Type B cores. The 2010 core showed increases of about 40% in paste cracking and microcracking, more than 50% increase in reaction rim microcracking, and 100% increase in aggregate debonding over the 2009 core.

4 DISCUSSION

The observations described above demonstrate that while both ACR and ASR are present in the subject concrete, the damage observed in the field is a result of ACR involving the Type A dolomitic limestone coarse aggregate. Furthermore, the results demonstrate the utility of using the DRI method to investigate the progression of damage within 18 months of exposure in the field. The observation that damage increased over this time span warranted significant concern for the owner regarding the integrity of the in-place concrete made with Type A coarse aggregate. Removal and replacement of all concrete made with Type A aggregate was recommended as the only measure to rehabilitate the structures at the facility. The analysis also showed that concrete made with the Type B aggregate showed no evidence of damage from ACR or ASR and that elements made with such concrete could be left in place. While minor ASR was observed in the cores, no damage was associated with it and no progression of distress was observed.

The results also showed the caution needed for taking results from accelerated exposure tests and applying them to actual field exposure conditions. The exposure test sample showed extensive aggregate pitting and deposits of gel in voids, but these features were negligible in both the field cores. This suggests that the accelerated test conditions triggered damage mechanisms unlikely to be encountered in the field. The increased pitting and gel formation was observed using a 0.5 N NaOH solution, which is half the concentration used in the ASTM C1260 test.

5 CONCLUSIONS

- Petrographic examination indicates that ACR is the primary damage mechanism affecting concrete made with dolomitic limestone coarse aggregate. Concrete made with calcitic limestones show no damage from ACR.
- While ASR is present and involves chert in the siliceous fine aggregate, it is negligible and has no association with any damage in the concrete.
- The DRI method provided a useful means to evaluate the extent of damage in cores and to determine if the severity of damage was increasing at a rate that warranted concern for the serviceability of the facility.
- The accelerated exposure testing triggered damage mechanisms that were not observed in the field, reinforcing the need to use results from such tests with caution.

6 REFERENCES

[1] Idorn, G.M. (1997): Concrete progress: from antiquity to the third millennium, Thomas Telford Publishing, London, pp 359.

[2] Multon, S., Sellier, A. And Cyr, M. (2009): Chemo-mechanical modeling for prediction of alkali-silica reaction (ASR) expansion, Cement and Concrete Research (39): 490-500.

[3] ASTM C856-11 (2011): Standard practice for petrographic examination of hardened concrete, American Society for Testing and Materials, West Conshoshocken, Annual Book of Standards (04.02), Concrete and Concrete Aggregates, pp 17.

[4] ASTM C457/C457M-10a (2010): Standard test method for microscopical determination of parameters of the air-void system in hardened concrete, American Society for Testing and Materials, West Conshoshocken, Annual Book of Standards (04.02), Concrete and Concrete Aggregates, pp 15.

[5] St. John, D.A., Poole, A.B., and Sims, I. (1998): Concrete petrography: a handbook of investigative techniques, Arnold Publishing, London, 474 pp.

[6] Grattan-Bellew, P.E. (1995): Laboratory evaluation of alkali-silica reaction in concrete from Saunders generating station, ACI Materials Journal (92): 126-134.

[7] Rivard, P., and Ballivy, G. (2005): Assessment of the expansion related to alkali-silica reaction by the Damage Rating Index method, Construction and Building Materials (19): 83-90.

[8] ASTM C1260-07 (2007): Standard test method for potential alkali reactivity of aggregates (mortar-bar method), American Society for Testing and Materials, West Conshoshocken, Annual Book of Standards (04.02), Concrete and Concrete Aggregates, pp 5.

Table 1. Summary of weights assigned to measured features for DRI method.

Measured Feature	Weight
Coarse aggregate with internal microcracks	x 0.25
Coarse aggregate with reaction rims	x 0.50
Coarse aggregate with microcracks in reaction rims	x 2
Coarse aggregate debonding	x 3
Fine aggregate with reaction rims	x 0.25
Fine aggregate pitting	x 0.25
Fine aggregate with internal microcracks	x 0.25
Gel in voids	x 0.50
Cracks and microcracks in paste	x 2

Figure 1. Photographs showing cracking damage observed in the field. (a) Exterior slab on ground showing map cracking. The field of view measures about 1.5 m across the bottom of the photograph. (b) Fence post footing with map cracking. The footing is about 46 cm in diameter.

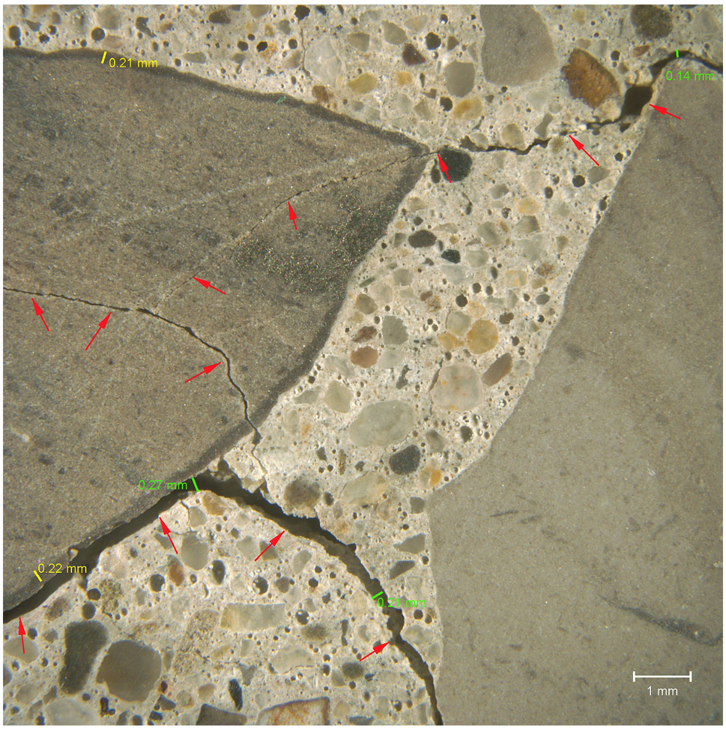

Figure 2. Reflected light photomicrographs of polished surface showing cracking and aggregate debonding associated with ACR. Red arrows indicate cracks and microcracks, green bars measure width of cracks and yellow bars measure width of reaction rim.

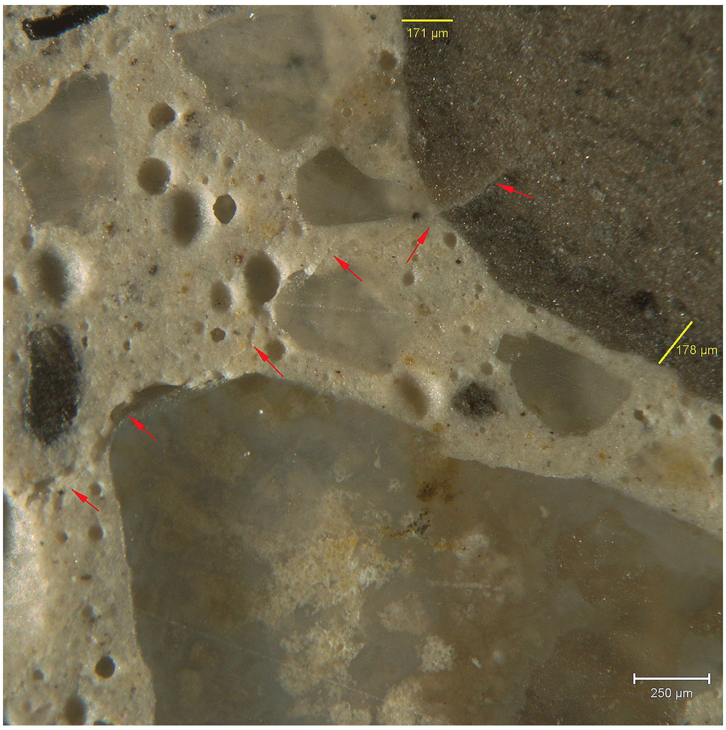

Figure 3. Reflected light photomicrographs of polished surface showing detail of microcrack (red arrows) in reaction rim (measured by yellow bars) that cuts into the paste.

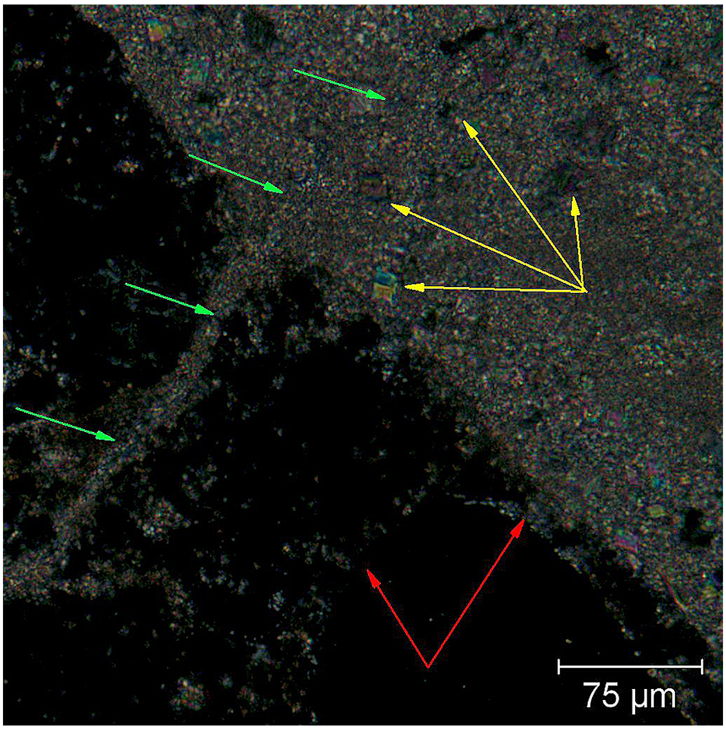

Figure 4. Cross-polarized transmitted light photomicrograph of thin section showing microcrack (green arrows) cutting from dolomitic limestone (brightly colored area) into the paste (dark area). The yellow arrows show dolomite rhombs and the red arrows highlight deposits of brucite in a void.

Figure 5. Reflected light photomicrograph of polished surface showing chert particle and rare microcracks associated with ASR. The white arrows show internal microcrack in the chert particle and the black arrows show microcracks filled with gel cutting the paste.

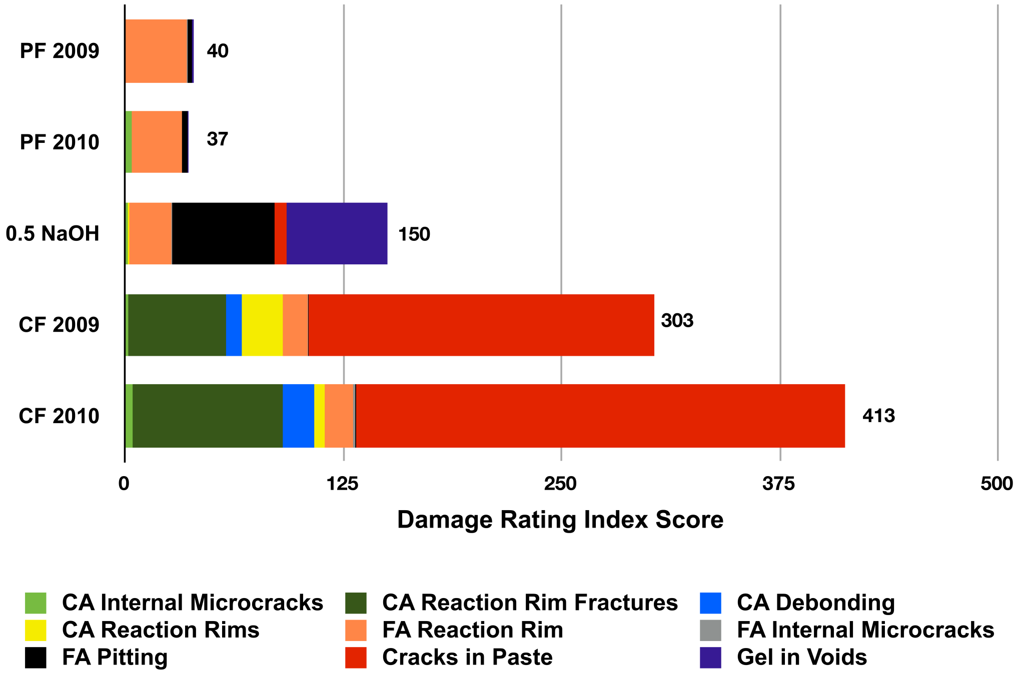

Figure 6. Bar chart summarizing the results of the DRI scores on the five samples described in the text. The samples are designated as follows. PF 2009 and PF 2010 are the perimeter footing cores taken in early 2009 and late 2010, respectively. 0.5 NaOH is the perimeter footing cored in early 2009 and subjected to accelerated exposure testing with 0.5 NaOH solution. CF 2009 and CF 2010 are the column footing cores taken in early 2009 and late 2010, respectively. CA and FA in the chart legend indicate coarse aggregate and fine aggregate, respectively.